Showcasing research from Professor Ágnes Vibók & Dr.
Csaba Fábri & Professor Lorenz S. Cederbaum's laboratories,
Department of Theoretical Physics, Department of Information
Technology, University of Debrecen, Debrecen (Hungary)
& Laboratory of Molecular Structure and Dynamics, Institute
of Chemistry, Eötvös Loránd University, Budapest (Hungary)
& Theoretische Chemie, Physikalish-Chemisches Institut,
Universität Heidelberg, Heidelberg (Germany).

Born–Oppenheimer approximation in optical cavities: from success
to breakdown

In this study, we discuss the applicability of the Born-Oppenheimer
approximation (BOA) in optical cavities for polyatomic molecules.
The formaldehyde molecule serves as a showcase example which
does not exhibit any natural nonadiabatic phenomena in the studied
energy region. By calculating the one-dimensional absorption
spectrum of the molecule, we could clearly identify the cavity-induced
nonadiabatic fingerprints, which appear solely due to light-matter
coupling, demonstrating that contrary to expectation, BOA may
even fail in a one-dimensional model. (Image by Gy. Bujdosó)

As featured in:

ROYAL SOCIETY
OF CHEMISTRY

rsc.li/chemical-science

Check for updates

Born–Oppenheimer approximation in optical cavities: from success to breakdown†

Csaba Fábri, [ID] *[ab] Gábor J. Halász, [ID] [c] Lorenz S. Cederbaum [ID] [d]
and Ágnes Vibók [ID] *[ef]

The coupling of a molecule and a cavity induces nonadiabaticity in the molecule which makes the description of its dynamics complicated. For polyatomic molecules, reduced-dimensional models and the use of the Born–Oppenheimer approximation (BOA) may remedy the situation. It is demonstrated that contrary to expectation, BOA may even fail in a one-dimensional model and is generally expected to fail in two- or more-dimensional models due to the appearance of conical intersections induced by the cavity.

1   Introduction

The dynamics initiated in a molecule by the absorption of a photon is usually treated within the framework of the Born–Oppenheimer (BO) or adiabatic approximation[1] where the fast-moving electrons are separated from the slow nuclear degrees of freedom (dofs). In this picture the nuclei move on a single potential energy surface (PES) created by the fast-moving electrons. Although several chemical processes can be rationalised by considering a single BO PES, there are indeed a number of situations where the BO approximation (BOA) breaks down. These are called nonadiabatic processes which involve nuclear dynamics proceeding on at least two coupled PESs, leading to the formation of so-called conical intersections (CIs).[2–7] Nonadiabatic phenomena are ubiquitous in photochemistry, photophysics, particularly in molecular fragmentation, proton transfer, isomerization or radiationless deactivation processes of excited states as the CI can provide a very efficient channel for ultrafast interstate crossing on the femtosecond timescale.[8–21]

Conical intersections and avoided crossings (ACs) can be created both by classical and quantum light, as well. To form a CI, the molecule must have at least two independent nuclear

dofs. In diatomics having only one nuclear dof, natural CIs can never be formed, only ACs can arise. If the system interacts with light, either light-induced avoided crossings (LIACs) or light-induced conical intersections (LICIs)[22–24] can emerge. LICIs can be created even in diatomics where the second dof (either rotation or translation), needed to form a LICI, comes into play due to the light-matter interaction. Moreover, LICIs are ubiquitous and become multidimensional in the nuclear coordinate space in polyatomic molecules due to the presence of several vibrational dofs.[25,26]

Recently, efforts have been made to study light-induced nonadiabatic phenomena in optical or microwave cavities.[27–46] It has been successfully demonstrated that describing the photon–matter interaction with the tools of cavity quantum electrodynamics (cQED)[47–50] can provide an alternative way to study the quantum control of molecules with light. In this framework nonadiabatic dynamics arises due to the strong coupling between the molecular dofs and the photonic mode of the radiation field which can alter the molecular energy levels by controlling the dynamics of basic photophysical and photochemical processes. The molecular vibrational modes which are strongly coupled to the electronic and photonic dofs are taken into account resulting in a new set of "cavity-induced" or "polariton" surfaces in the molecular Hamiltonian. These polariton surfaces are expected to form LIACs or LICIs.

Numerous works deal with quantum-light-induced nonadiabatic effects within a single molecule. In most of the studies diatomic or polyatomic organic molecules are treated as reduced-dimensional two-level systems by taking into account only one vibrational and photonic dof.[27–29,34,35,42] As is already clear from classical light, quantum LICI situations can also only occur if, in addition to the only vibrational dof, the rotational angle between the molecular axis and the polarization vector of the electric field in the cavity is also accounted for (in case of diatomics)[37,38] or at least two vibrational dofs are considered in

[a]Laboratory of Molecular Structure and Dynamics, Institute of Chemistry, Eötvös Loránd University, Pázmány Péter sétány 1/A, H-1117 Budapest, Hungary. E-mail: ficsaba@caesar.elte.hu

[b]MTA-ELTE Complex Chemical Systems Research Group, P.O. Box 32, H-1518 Budapest, Hungary

[c]Department of Information Technology, University of Debrecen, P.O. Box 400, H-4002 Debrecen, Hungary

[d]Theoretische Chemie, Physikalisch-Chemisches Institut, Universität Heidelberg, Im Neuenheimer Feld 229, 69120 Heidelberg, Germany

[e]Department of Theoretical Physics, University of Debrecen, PO Box 400, H-4002 Debrecen, Hungary. E-mail: vibok@phys.unideb.hu

[f]ELI-ALPS, ELI-HU Non-Profit Ltd, Dugonics tér 13, H-6720 Szeged, Hungary

† Electronic supplementary information (ESI) available. See DOI: 10.1039/d0sc05164k

the description.[26,44] Furthermore, quantum light-induced collective nonadiabatic phenomena (collective LICI) can also emerge when many molecules are involved in strong coupling to the cavity mode.[34,35,42]

Our current aim is to study pure quantum light-induced nonadiabatic phenomena in a single polyatomic molecule placed in an optical nanocavity with methods ranging from a full-dimensional and accurate quantum-dynamical description to a simple one-dimensional treatment. In order to eliminate any possible interference between inherent and cavity-induced nonadiabatic phenomena, we consider situations where a clear separation and identification of these can be made, enabling us to reveal effects solely caused by the quantum LICI.

Our showcase example is the four-atomic H_2CO (formaldehyde) molecule which has been investigated very recently for nonadiabatic phenomena induced by classical light.[26] This molecule does not exhibit any inherent nonadiabatic effects in the studied region of the nuclear configuration space (see

description of H_2CO, irrespective of the coupling strength. Consequently, BOA is expected to fail in the presence of a LICI and care should be taken when a molecule coupled to a cavity mode is described using the BOA with only one vibrational dof.

2 Results and discussion

2.1 Hamiltonian of a single molecule coupled to a cavity mode and six-dimensional results

Let us start with the Hamiltonian of a single molecule coupled to a cavity mode,[51]

$$\hat{H} = \hat{H}_0 + \hbar\omega_c\hat{a}^\dagger\hat{a} - g\vec{\hat{\mu}}\vec{e}(\hat{a}^\dagger + \hat{a}) \tag{1}$$

where $\hat{H}_0$ denotes the Hamiltonian of the isolated molecule, $\vec{\hat{\mu}}$ is the electric dipole moment operator, $\vec{e}$ is the polarization vector, $\hat{a}^\dagger$ and $\hat{a}$ are the creation and annihilation operators of the cavity mode, ω_c is the angular frequency of the cavity mode and g is the coupling strength parameter. If two electronic states of the molecule are considered, the Hamiltonian takes the form

$$\hat{H} = \begin{bmatrix} \hat{T} + V_X & 0 & 0 & W_1 & 0 & 0 & \dots \\ 0 & \hat{T} + V_A & W_1 & 0 & 0 & 0 & \dots \\ 0 & W_1 & \hat{T} + V_X + \hbar\omega_c & 0 & 0 & W_2 & \dots \\ W_1 & 0 & 0 & \hat{T} + V_A + \hbar\omega_c & W_2 & 0 & \dots \\ 0 & 0 & 0 & W_2 & \hat{T} + V_X + 2\hbar\omega_c & 0 & \dots \\ 0 & 0 & W_2 & 0 & 0 & \hat{T} + V_A + 2\hbar\omega_c & \dots \\ \vdots & \vdots & \vdots & \vdots & \vdots & \vdots & \ddots \end{bmatrix} \tag{2}$$

further explanation in ESI†). Therefore, nonadiabatic effects appearing in the absorption spectrum of H_2CO coupled to a single cavity mode can be attributed solely to the quantum LICI. First, by applying accurate full-dimensional computations, the field-free absorption spectrum of H_2CO is investigated and compared to results obtained with one- and two-dimensional quantum-dynamical models. Next, we study the absorption spectrum of H_2CO coupled to a single cavity mode and investigate how cavity-induced nonadiabatic phenomena can be understood if simplified one- and two-dimensional descriptions are used. Most importantly, we examine whether the BOA is capable of yielding qualitatively (or even quantitatively) correct absorption spectra for the different quantum-dynamical models applied in this study.

The BOA, to be accurately defined later in the context of polaritonic surfaces, breaks down for both the two- and six-dimensional quantum-dynamical models used in this work. The failure of the BOA is attributed to the emergence of the LICI between polaritonic surfaces. However, if only one vibrational dof is taken into account, no LICI can be formed and it seems plausible that the BOA can provide correct absorption spectra. In ref. 27 it has been found that the BOA is valid for larger organic molecules described in one dimension provided that the coupling between the molecule and the cavity mode is sufficiently strong. The most striking outcome of the present work is that the BOA can fail even for a one-dimensional

where $\hat{T}$ is the kinetic energy operator, V_X and V_A denote the ground-state and excited-state PESs and $W_n = -g\sqrt{n}\vec{\mu}\vec{e}$, where $\vec{\mu}$ is the transition dipole moment (TDM) vector. In what follows, the notation $\mu = \vec{\mu}\vec{e}$ will be used.

The eigenstates of the Hamiltonian of eqn (2)

$$|\Phi_k\rangle = \sum_{\alpha=X,A}\sum_i\sum_n c_{\alpha in}^{(k)}|\alpha i\rangle|n\rangle \tag{3}$$

can be obtained as the linear combination of the products of field-free molecular vibronic eigenstates (denoted by $|Xi\rangle$ and $|Ai\rangle$) and Fock states $|n\rangle$ ($n = 0, 1, 2,\dots$) of the cavity mode. The intensities of electric dipole transitions between the eigenstates $|\Phi_k\rangle$ and $|\Phi_l\rangle$ are expressed as

$$I_{kl} \propto \omega_{kl}\sum_{\alpha=x,y,z}|\langle\Phi_k|\hat{\mu}_\alpha|\Phi_l\rangle|^2 \tag{4}$$

where ω_{kl} is the angular frequency of the transition and $\hat{\mu}_\alpha$ denotes the components of the electric dipole moment operator.

Following the footsteps of our previous study focused on light-induced nonadiabaticity in polyatomic molecules,[26] we choose the four-atomic H_2CO molecule as the target of the present work. The two singlet electronic states S_0 ($\tilde{X}\,^1A_1$) and S_1 ($\tilde{A}\,^1A_2$) of H_2CO are taken into account and the corresponding six-dimensional V_X and V_A PESs are taken from ref. 52 and 53, respectively. The structure of H_2CO coupled to a single cavity

mode and the three lowest polaritonic (adiabatic) PESs that emerge due to the light–matter coupling are depicted in Fig. 1. The field-free vibrational eigenstates of H_2CO were computed with the GENIUSH program package[54–56] for both electronic states treating all six vibrational dofs in a numerically exact way. The rotational dofs are omitted from the present computational protocol and the molecule is imagined to be fixed with respect to the external electric field. Further information on the structure and normal modes of H_2CO as well as technical details of the computations are provided in the ESI.†

Having described the working formulae and the molecular system, we move on to the discussion of the absorption spectrum of the field-free H_2CO molecule and first present results with a numerically-exact six-dimensional (6D) quantum-dynamical treatment. We consider the high-energy part of the spectrum consisting of spectral lines corresponding to transitions from $|X0\rangle$ (vibrational ground state of the electronic state X) to $|Ai\rangle$ (vibrational states of the electronic state A). Fig. 2 presents the 6D field-free spectrum of H_2CO, showing favourable agreement with results reported in ref. 57. The 6D field-free spectrum exhibits progressions of lines that are mainly associated with the ν_4 (out-of-plane bend) and ν_2 (C=O stretch)
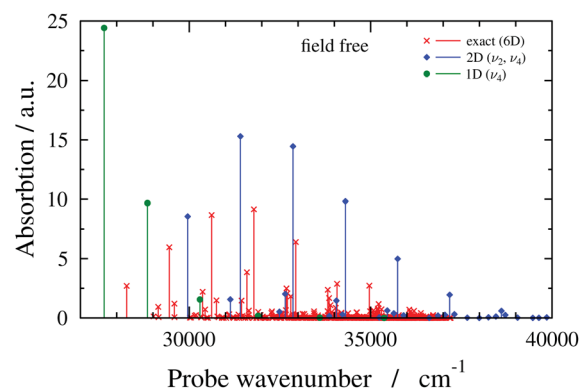

Fig. 2 Absorption spectra of field-free (i.e., no cavity) formaldehyde obtained with different quantum-dynamical models (6D, 2D(ν_2,ν_4) and 1D(ν_4) models, as indicated in the figure).

vibrational modes. Displacements along the ν_4 vibrational mode produce nonzero TDM and since the C=O equilibrium bond length in the excited electronic state is considerably larger than the corresponding ground-state value, the ν_2 vibrational mode adds complexity to the absorption spectrum by giving rise to several nonzero Franck–Condon factors. Therefore, any reduced-dimensional quantum-dynamical model of H_2CO should incorporate at least the ν_4 and ν_2 vibrational modes. However, if one still aims to define a one-dimensional model, the ν_2 vibrational mode should be omitted as explained in the next paragraph.

Fig. 2 also shows field-free spectra obtained with two reduced-dimensional models, treating the ν_2 and ν_4 vibrational modes (2D(ν_2,ν_4) model), or the ν_4 vibrational mode (1D(ν_4) model). Comparing the field-free 2D(ν_2,ν_4) spectrum to its 6D counterpart reveals that although the 2D(ν_2,ν_4) spectrum lacks lines that are present in the 6D spectrum, the overall structures of the 2D(ν_2,ν_4) and 6D field-free spectra are similar. On the contrary, the 1D(ν_4) field-free spectrum does not resemble the 6D field-free spectrum at all. Besides the 1D(ν_4) model, one could also think of testing the performance of the 1D(ν_2) model. Since the reduced-dimensional models are defined by setting the inactive normal coordinates to zero and the ν_2 vibrational mode is totally symmetric, the C_{2v} symmetry of the equilibrium structure is preserved when displacements are made along the ν_2 vibrational mode (see also ESI†). Due to symmetry, the TDM between the electronic states X and A is zero at nuclear configurations of C_{2v} symmetry, therefore, no transitions are allowed if the 1D(ν_2) model is used. Based on the analysis of the field-free spectra presented in this subsection, the simplest model expected to provide sensible results is the 2D(ν_2,ν_4) model.

2.2 One-dimensional results for the 1D(ν_4) model

We define a one-dimensional quantum-dynamical model, called 1D(ν_4) model henceforth, treating only the ν_4 (out-of-plane) vibrational mode of H_2CO (see ESI† for technical details). The 1D(ν_4) model is utilized to assess the performance of a simplified one-dimensional description for H_2CO and test
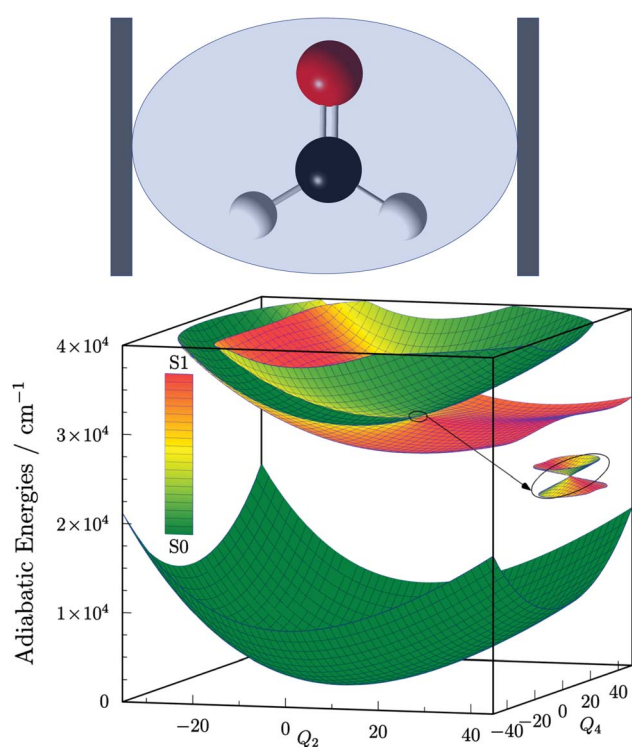

Fig. 1 Structure of the H_2CO (formaldehyde) molecule (upper panel) and the three lowest polaritonic (adiabatic) surfaces of H_2CO coupled to a single cavity mode (lower panel). Q_2 and Q_4 are the normal coordinates of the ν_2 (C=O stretch) and ν_4 (out-of-plane bend) vibrational modes. The cavity wavenumber and coupling strength are chosen as $\omega_c = 29\,000$ cm^{-1} and $g = 5.97 \times 10^{-2}$ a.u., respectively. The light-induced conical intersection between the second and third polaritonic surfaces is shown in the inset on the right-hand side of the lower panel. The character of the polaritonic surfaces is indicated by different colours (see the legend on the left).
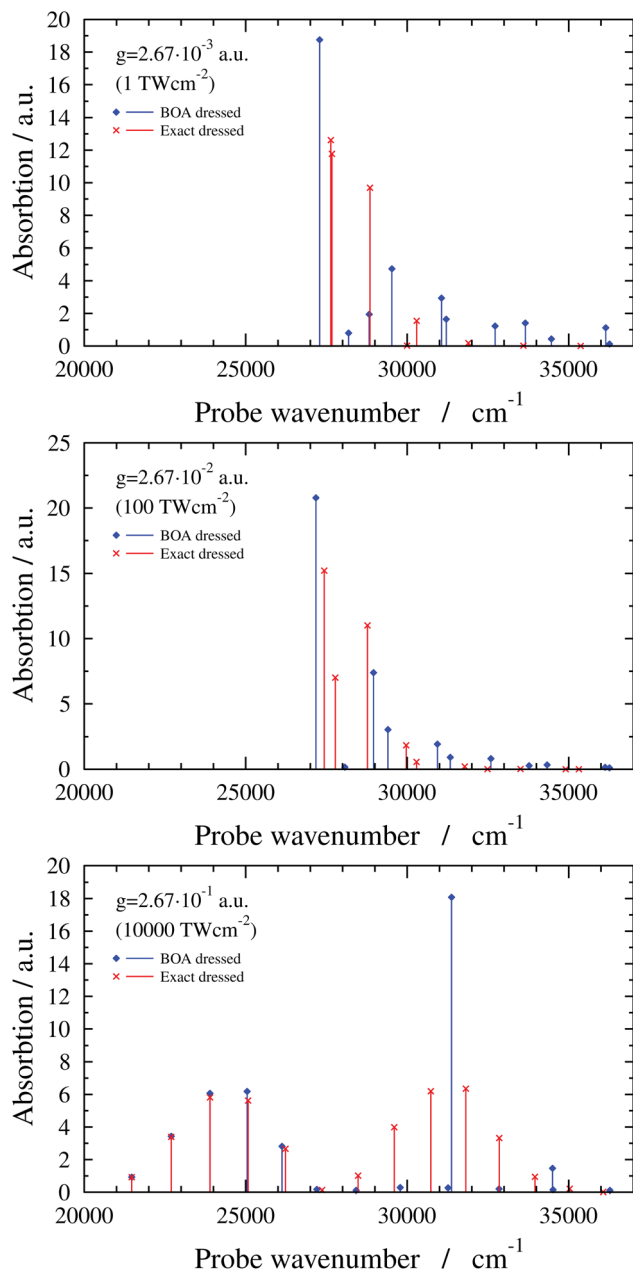
Fig. 3 1D(ν_4) dressed spectra (exact and BOA) with a cavity wavenumber of $\omega_c = 27\,653.3$ cm^{-1} for different coupling strength values.
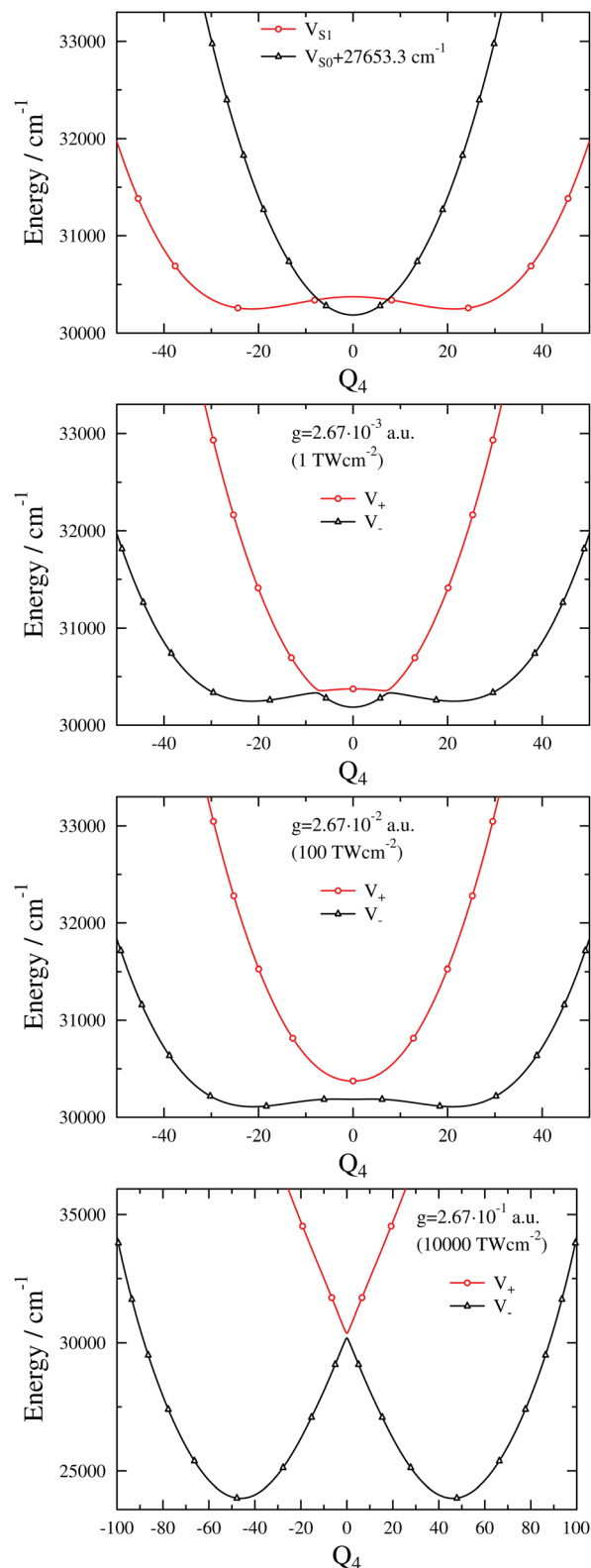

Fig. 4 1D(ν_4) diabatic (uppermost panel) and adiabatic potential curves (V_+ and V_-) with a cavity wavenumber of $\omega_c = 27\,653.3$ cm^{-1} for different coupling strength values. Note that the range of the energy axis in the last panel ($g = 2.67 \times 10^{-1}$ a.u.) differs from those of the other three panels.

the applicability of the BOA in one dimension, which requires further explanation. Since the frequency of the cavity mode is chosen to be nearly resonant with the frequency of the X → A electronic excitation, the dof associated with the "fast" cavity mode is grouped with the electrons and the "slow" nuclear dofs are separated from the electronic and cavity dofs. This allows the construction of the lower ($|-\rangle$) and upper ($|+\rangle$) hybrid light-matter (polaritonic) states that can be approximately described as

$$|-\rangle = a|X\rangle|1\rangle - b|A\rangle|0\rangle$$
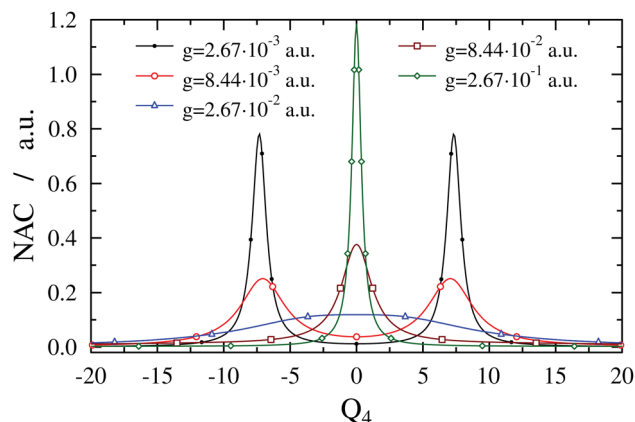$$|+\rangle = b|X\rangle|1\rangle + a|A\rangle|0\rangle \qquad (5)$$

Fig. 5 Nonadiabatic coupling (1D(ν_4) model) as a function of Q_4 for formaldehyde in a cavity of $\omega_c = 27\,653.3$ cm^{-1} with different coupling strength values g. With growing coupling strength, the bimodal structure of the nonadiabatic coupling turns into a single maximum following the structure of the avoided crossings of the adiabatic potentials shown in Fig. 4.

in the singly-excited subspace. The corresponding polaritonic (adiabatic) PESs can be obtained as eigenvalues of the potential energy part of the Hamiltonian of eqn (2) at each nuclear configuration. Throughout this work, the BOA is defined by neglecting the nonadiabatic coupling (NAC) between the lower and upper polaritonic PES (V_- and V_+). Next, the absorption spectrum is computed using the BOA and the BOA spectrum is compared to the exact absorption spectrum that includes all effects caused by the NAC. Note that all spectra presented in this subsection have been calculated utilizing the 1D(ν_4) model.

The initial dressed state $|\Phi_i\rangle$ is always chosen as the lowest-energy dressed state. As for the current range of g the lowest polariton PES (see the first polariton PES in Fig. 1) can be approximated as V_X (strong coupling regime), $|\Phi_i\rangle$ virtually equals $|X0\rangle|0\rangle$, that is, the product of $|X0\rangle$ and the vacuum state of the cavity mode. The final dressed states $|\Phi_f\rangle$ of the transitions lie in the singly-excited subspace (molecule in ground electronic state X dressed with one photon or molecule in excited electronic state A dressed with zero photon). Note that the second and third polaritonic PESs in Fig. 1 correspond to the singly-excited subspace. We stress that in the numerical computations all coupling terms appearing in the Hamiltonian of eqn (2) are included explicitly.

The exact dressed spectra displayed in Fig. 3 ($\omega_c = 27\,653.3$ cm^{-1} and $e = (0, 1, 0)$ with different values of g) show the emergence of new peaks besides splittings and shifts of peaks that are present in the field-free spectrum. It is apparent in Fig. 3 that the dressed spectra calculated using the BOA are rather different from their exact counterparts for all g values considered. The lower panel in Fig. 3 shows the dressed spectrum with $g = 2.67 \times 10^{-1}$ a.u. (equivalent to a classical intensity of $I = 10\,000$ TW cm^{-2}), the highest (and likely experimentally not yet feasible) value of g applied. In contrast to the dressed spectra with lower g values, the spectrum with $g = 2.67 \times 10^{-1}$ a.u. exhibits two clearly separated groups of peaks. Moreover, it is conspicious that the BOA works for

the lower group of peaks and fails completely for the upper group of peaks in this particular case.

The breakdown of the BOA even for the highest g value might seem counterintuitive as only one vibrational dof is taken into account. In order to rationalise this odd result we have investigated the lower and upper polaritonic (adiabatic) PESs and evaluated the NAC for several g values. Fig. 4 displays both the diabatic ($V_X + \hbar\omega_c$ and V_A) and adiabatic PESs (V_- and V_+) as a function of the ν_4 normal coordinate (Q_4). The diabatic PESs cross at $Q_4 = \pm 7.35$ and $30\,344.8$ cm^{-1} for $\omega_c = 27\,653.3$ cm^{-1}. Note that V_A shows an anharmonic double-well structure and

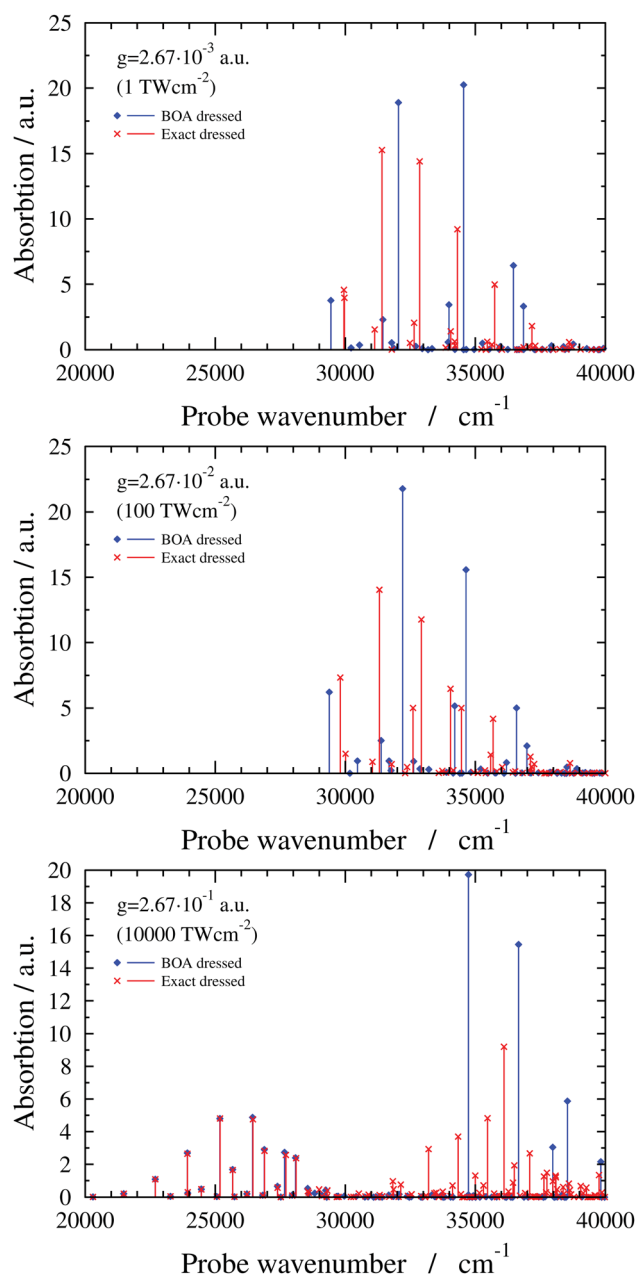**Fig. 6** 2D(ν_2, ν_4) dressed spectra (exact and BOA) with a cavity wavenumber of $\omega_c = 29\,957.23$ cm^{-1} for different coupling strength values.

the TDM vanishes at $Q_4 = 0$ due to symmetry, which implies that the gap between V_- and V_+ at $Q_4 = 0$ is determined solely by ω_c (and not by g). One can also observe LIACs in Fig. 4 and the shapes of V_- and V_+ change substantially as g increases. An interesting feature of V_- is the emergence of a barrier centered at $Q_4 = 0$ for high g values. Fig. 5 shows the NAC as a function of Q_4 for several g values. One can notice in Fig. 5 that at lower g values the NAC curve has a bimodal structure (with maxima located around the two crossing points of the diabatic PESs), while at higher g values the NAC exhibits a single maximum at $Q_4 = 0$. This behaviour of the NAC can be qualitatively interpreted by examining the shape of the adiabatic PES. While at lower g values the adiabatic PESs show two LIACs around the crossing points of the diabatic PESs, at higher g values the adiabatic PES show only one LIAC at $Q_4 = 0$. The shape of the NAC curve follows this trend and the bimodal NAC curve (lower g values) turns into a unimodal NAC curve centered at $Q_4 = 0$ (higher g values).

The numerical NAC results can be quantitatively understood by a simple one-dimensional model with two harmonic PESs,

$$V_X(x) = \frac{1}{2} m \omega_X^2 x^2$$
$$V_A(x) = \frac{1}{2} m \omega_A^2 x^2 + \Delta, \tag{6}$$

coupled by a linear TDM,

$$\mu(x) = \alpha x, \tag{7}$$

which, similarly to the TDM of the 1D(v_4) model, vanishes at $x = 0$. In eqn (6) m is the mass of the oscillator, ω_X and ω_A refer to the harmonic frequencies of the ground and excited electronic states and Δ denotes the excitation energy. Although the 1D(v_4) V_A PES has an anharmonic double-well structure, we believe that the harmonic approximation for V_A still yields a correct interpretation of the g-dependence of the NAC. As the NAC(x) formula is rather involved (see ESI† for details of the analytical derivations), here the NAC is evaluated only at the two crossing points of the two diabatic PESs (x_0), that is,

$$\text{NAC}(x_0) = \frac{m(\omega_X^2 - \omega_A^2)}{4g\alpha} \propto g^{-1}, \tag{8}$$

and at $x = 0$, where one gets

$$\text{NAC}(0) = \frac{g\alpha}{\Delta - \hbar\omega_c} \propto g. \tag{9}$$

While eqn (8) shows that the NAC is inversely proportional to g around x_0, implying that the NAC becomes negligible for sufficiently large g values in this region, eqn (9) clearly indicates that the NAC is proportional to g at $x = 0$. This striking behaviour of the NAC provides an explanation for the shape of the NAC curves in Fig. 5 and indicates that the BOA indeed breaks down even for large g values in the 1D(v_4) model.

Finally, the interpretation of the partial BOA breakdown for the highest value of g (2.67×10^{-1} a.u.) is in order. The analysis of the dressed spectrum reveals that the peaks of the lower group in the BOA spectrum (see lower panel in Fig. 3) correspond to transitions to the lower-lying eigenstates of V_-. Since

V_- exhibits a high barrier in this case (see last panel in Fig. 4), the lower-lying adiabatic eigenstates of V_- have negligible amplitude around $Q_4 = 0$, i.e., in the region where the NAC is not negligible according to Fig. 5. Therefore, the BOA provides satisfactory results for the lower group of peaks. As to the higher group of peaks, the final dressed states of these BOA transitions are adiabatic eigenstates of V_+ which has a single minimum at $Q_4 = 0$, therefore, the effect of the NAC can not be neglected and the BOA breaks down.

Interestingly, the higher group of states can be explained by the potential curve obtained by connecting smoothly the left (right) part of V_+ with the right (left) part of V_- in the last panel of Fig. 4. The resulting curves can be viewed as diabatic curves and their diabatic coupling is weak as the energy gap at $Q_4 = 0$ is small.

2.3 Two-dimensional results for the 2D(v_2,v_4) model

In this subsection results are presented for a two-dimensional quantum-dynamical model, referred to as the 2D(v_2,v_4) model, treating both the v_2 and v_4 vibrational modes (see ESI† for technical details). Fig. 6 shows 2D(v_2,v_4) dressed spectra ($\omega_c = 29\,957.23$ cm^{-1} and $\boldsymbol{e} = (0, 1, 0)$ with different g values). The exact dressed spectrum for the lowest value of g in Fig. 6 shows splitting of the first band of the field-free spectrum. As g increases, further field-free lines become split and shifted, and new lines appear. Common to all g values is that the BOA and exact dressed spectra differ substantially. At the highest value of g one can again observe the emergence of two groups of peaks in the dressed spectrum. In this case the BOA again works well for the lower group of peaks and utterly breaks down for the upper group of peaks.

The breakdown of the BOA in case of the 2D(v_2,v_4) model can be attributed to the LICI, also visible in Fig. 1. For $\omega_c = 29\,957.23$ cm^{-1}, the LICI is located at an energy of 30 776.1 cm^{-1} at $Q_2 = 8.84$ and $Q_4 = 0$. V_- and V_+ are degenerate at the LICI and the NAC becomes singular, also verified by analytical 2D model calculations described in the ESI.† Similarly to the 1D(v_4) case, the final states of the BOA transitions in the lower group of peaks for $g = 2.67 \times 10^{-1}$ a.u. are lower-lying V_- adiabatic eigenstates which have negligible amplitude at the LICI. On the other hand, BOA lines in the upper group of peaks correspond to transitions to either higher-lying V_- adiabatic eigenstates that are above the LICI in energy or to adiabatic eigenstates of V_+ which has a minimum at the LICI. Therefore, the BOA can not be expected to yield sensible results for the upper group of peaks. Note that similar conclusions have been drawn for natural CIs.[2,58] Along these lines, we believe that the BOA fails for the 6D model, similarly to the 2D(v_2,v_4) model, due to the presence of the LICI.

3 Conclusions

This study discusses the applicability of the Born–Oppenheimer approximation (BOA) in optical cavities for polyatomic molecules. The H$_2$CO molecule serves as a showcase example and its absorption spectrum is calculated for the energy region of electronic transitions. H$_2$CO does not exhibit a natural conical intersection in the studied energy region, and therefore,

nonadiabatic effects appearing in the absorption spectrum can be attributed solely to the quantum LICI.

First, as for comparison, we have calculated the field-free spectrum of H_2CO utilizing the full-dimensional (6D) as well as reduced-dimensional (2D(v_2, v_4) and 1D(v_4)) quantum-dynamical models. It has been found that the simplest model which can approximately reproduce the structure of the numerically-exact 6D spectrum is the 2D(v_2, v_4) model. As the one-dimensional 1D(v_2) model leads to a vanishing absorption spectrum, the 1D(v_4) model is the one-dimensional model to be used.

For the reduced-dimensional 1D(v_4) and 2D(v_2, v_4) models, the field-dressed exact and BOA spectra have been computed and compared. A striking finding of our work is that the BOA can fail even for a one-dimensional quantum-dynamical treatment of H_2CO irrespective of the value of the coupling strength. This complements previous results claiming that the BOA can be used in the strong coupling regime when only one vibrational dof is taken into account. Analytical considerations fully corroborate our conclusion and point out that the breakdown of the BOA even in 1D for H_2CO arises due to an intrinsic property of the molecule, namely that the transition dipole moment vanishes at certain geometries due to molecular symmetry. Clearly, one should be careful even when describing a molecule in a cavity using the BOA with only one vibration.

Moreover, we have also shown that the BOA is not applicable for the 2D(v_2, v_4) model. We can expect such a failure whenever there is a LICI and the spectrum extends to energies above the LICI. Consequently, we have no doubt that the BOA fails for the full-dimensional (6D) model as well.

The above-discussed aspects are valid when the system under investigation lacks any inherent nonadiabatic phenomena in the absence of the cavity. If this is not the case, the situation is expected to be even more involved.

Conflicts of interest

There are no conflicts to declare.

Acknowledgements

Notes and references

1 M. Born and R. Oppenheimer, *Ann. Phys.*, 1927, **389**, 457–484.
2 H. Köppel, W. Domcke and L. S. Cederbaum, *Adv. Chem. Phys.*, 1984, **57**, 59–246.
3 D. R. Yarkony, *Rev. Mod. Phys.*, 1996, **68**, 985–1013.
4 M. Baer, *Phys. Rep.*, 2002, **358**, 75–142.
5 G. A. Worth and L. S. Cederbaum, *Annu. Rev. Phys. Chem.*, 2004, **55**, 127–158.
6 W. Domcke, D. R. Yarkony and H. Köppel, *Conical Intersections*, World Scientific, 2004.
7 M. Baer, *Beyond Born–Oppenheimer: Electronic Non-Adiabatic Coupling Terms and Conical Intersections*, Wiley, New York, 2006.
8 J. S. Lim and S. K. Kim, *Nat. Chem.*, 2010, **2**, 627–632.
9 H. J. Wörner, J. B. Bertrand, B. Fabre, J. Higuet, H. Ruf, A. Dubrouil, S. Patchkovskii, M. Spanner, Y. Mairesse, V. Blanchet, E. Mével, E. Constant, P. B. Corkum and D. M. Villeneuve, *Science*, 2011, **334**, 208–212.
10 H. S. You, S. Han, J. S. Lim and S. K. Kim, *J. Phys. Chem. Lett.*, 2015, **6**, 3202–3208.
11 A. J. Musser, M. Liebel, C. Schnedermann, T. Wende, T. B. Kehoe, A. Rao and P. Kukura, *Nat. Phys.*, 2015, **11**, 352–357.
12 A. von Conta, A. Tehlar, A. Schletter, Y. Arasaki, K. Takatsuka and H. J. Wörner, *Nat. Commun.*, 2018, **9**, 3162.
13 M. E. Corrales, J. González-Vázquez, R. de Nalda and L. Bañares, *J. Phys. Chem. Lett.*, 2019, **10**, 138–143.
14 T. J. Martinez, *Nature*, 2010, **467**, 412–413.
15 C. Xie, J. Ma, X. Zhu, D. R. Yarkony, D. Xie and H. Guo, *J. Am. Chem. Soc.*, 2016, **138**, 7828–7831.
16 J. A. DeVine, M. L. Weichman, X. Zhou, J. Ma, B. Jiang, H. Guo and D. M. Neumark, *J. Am. Chem. Soc.*, 2016, **138**, 16417–16425.
17 K. C. Woo, D. H. Kang and S. K. Kim, *J. Am. Chem. Soc.*, 2017, **139**, 17152–17158.
18 B. F. E. Curchod and T. J. Martínez, *Chem. Rev.*, 2018, **118**, 3305–3336.
19 K. Bennett, M. Kowalewski, J. R. Rouxel and S. Mukamel, *Proc. Natl. Acad. Sci. U. S. A.*, 2018, **115**, 6538–6547.
20 I. G. Ryabinkin, L. Joubert-Doriol and A. F. Izmaylov, *Acc. Chem. Res.*, 2017, **50**, 1785–1793.
21 C. Xie, C. L. Malbon, H. Guo and D. R. Yarkony, *Acc. Chem. Res.*, 2019, **52**, 501–509.
22 N. Moiseyev, M. Šindelka and L. S. Cederbaum, *J. Phys. B: At., Mol. Opt. Phys.*, 2008, **41**, 221001.
23 G. J. Halász, A. Vibók and L. S. Cederbaum, *J. Phys. Chem. Lett.*, 2015, **6**, 348–354.
24 A. Csehi, G. J. Halász, L. S. Cederbaum and A. Vibók, *J. Phys. Chem. Lett.*, 2017, **8**, 1624–1630.
25 P. V. Demekhin and L. S. Cederbaum, *J. Chem. Phys.*, 2013, **139**, 154314.
26 C. Fábri, B. Lasorne, G. J. Halász, L. S. Cederbaum and Á. Vibók, *J. Phys. Chem. Lett.*, 2020, **11**, 5324–5329.
27 J. Galego, F. J. Garcia-Vidal and J. Feist, *Phys. Rev. X*, 2015, **5**, 041022.
28 M. Kowalewski, K. Bennett and S. Mukamel, *J. Phys. Chem. Lett.*, 2016, 7, 2050–2054.
29 H. L. Luk, J. Feist, J. J. Toppari and G. Groenhof, *J. Chem. Theory Comput.*, 2017, **13**, 4324–4335.
30 J. Flick, M. Ruggenthaler, H. Appel and A. Rubio, *Proc. Natl. Acad. Sci. U. S. A.*, 2017, **114**, 3026–3034.
31 J. Flick, H. Appel, M. Ruggenthaler and A. Rubio, *J. Chem. Theory Comput.*, 2017, **13**, 1616–1625.

32 M. Du, L. A. Martínez-Martínez, R. F. Ribeiro, Z. Hu, V. M. Menon and J. Yuen-Zhou, *Chem. Sci.*, 2018, **9**, 6659–6669.

33 R. F. Ribeiro, L. A. Martínez-Martínez, M. Du, J. Campos-Gonzalez-Angulo and J. Yuen-Zhou, *Chem. Sci.*, 2018, **9**, 6325–6339.

34 J. Feist, J. Galego and F. J. Garcia-Vidal, *ACS Photonics*, 2018, **5**, 205–216.

35 O. Vendrell, *Phys. Rev. Lett.*, 2018, **121**, 253001.

36 J. F. Triana, D. Peláez and J. L. Sanz-Vicario, *J. Phys. Chem. A*, 2018, **122**, 2266–2278.

37 T. Szidarovszky, G. J. Halász, A. G. Császár, L. S. Cederbaum and A. Vibók, *J. Phys. Chem. Lett.*, 2018, **9**, 6215–6223.

38 A. Csehi, M. Kowalewski, G. J. Halász and Á. Vibók, *New J. Phys.*, 2019, **21**, 093040.

39 J. B. Pérez-Sánchez and J. Yuen-Zhou, *J. Phys. Chem. Lett.*, 2019, **11**, 152–159.

40 A. Mandal and P. Huo, *J. Phys. Chem. Lett.*, 2019, **10**, 5519–5529.

41 M. Litinskaya and F. Herrera, *Phys. Rev. B*, 2019, **99**, 041107.

42 I. S. Ulusoy, J. A. Gomez and O. Vendrell, *J. Phys. Chem. A*, 2019, **123**, 8832–8844.

43 J. F. Triana and J. L. Sanz-Vicario, *Phys. Rev. Lett.*, 2019, **122**, 063603.

44 B. Gu and S. Mukamel, *Chem. Sci.*, 2020, **11**, 1290–1298.

45 F. Herrera, *Chem*, 2020, **6**, 7–9.

46 A. Mandal, T. D. Krauss and P. Huo, *J. Phys. Chem. B*, 2020, **124**, 6321–6340.

47 J. A. Hutchison, T. Schwartz, C. Genet, E. Devaux and T. W. Ebbesen, *Angew. Chem., Int. Ed.*, 2012, **51**, 1592–1596.

48 T. W. Ebbesen, *Acc. Chem. Res.*, 2016, **49**, 2403–2412.

49 R. Chikkaraddy, B. De Nijs, F. Benz, S. J. Barrow, O. A. Scherman, E. Rosta, A. Demetriadou, P. Fox, O. Hess and J. J. Baumberg, *Nature*, 2016, **535**, 127–130.

50 X. Zhong, T. Chervy, S. Wang, J. George, A. Thomas, J. A. Hutchison, E. Devaux, C. Genet and T. W. Ebbesen, *Angew. Chem., Int. Ed.*, 2016, **128**, 6310–6314.

51 C. Cohen-Tannoudji, J. Dupont-Roc and G. Grynberg, *Atom-Photon Interactions: Basic Processes and Applications*, Wiley-VCH Verlag GmbH and Co. KGaA, Weinheim, 2004.

52 X. Wang, P. L. Houston and J. M. Bowman, *Philos. Trans. R. Soc., A*, 2017, **375**, 20160194.

53 B. Fu, B. C. Shepler and J. M. Bowman, *J. Am. Chem. Soc.*, 2011, **133**, 7957–7968.

54 E. Mátyus, G. Czakó and A. G. Császár, *J. Chem. Phys.*, 2009, **130**, 134112.

55 C. Fábri, E. Mátyus and A. G. Császár, *J. Chem. Phys.*, 2011, **134**, 074105.

56 A. G. Császár, C. Fábri, T. Szidarovszky, E. Mátyus, T. Furtenbacher and G. Czakó, *Phys. Chem. Chem. Phys.*, 2012, **14**, 1085–1106.

57 M. Bonfanti, J. Petersen, P. Eisenbrandt, I. Burghardt and E. Pollak, *J. Chem. Theory Comput.*, 2018, **14**, 5310–5323.

58 L. S. Cederbaum, H. Köppel and W. Domcke, *Int. J. Quantum Chem.*, 1981, **20**, 251–267.